

UC Davis

UC Davis Previously Published Works

Title

Cerebral tract integrity relates to white matter hyperintensities, cortex volume, and cognition

Permalink

<https://escholarship.org/uc/item/9k10310x>

Authors

Seiler, Stephan
Fletcher, Evan
Hassan-Ali, Kinsy
et al.

Publication Date

2018-12-01

DOI

10.1016/j.neurobiolaging.2018.08.005

Peer reviewed



Published in final edited form as:

Neurobiol Aging. 2018 December ; 72: 14–22. doi:10.1016/j.neurobiolaging.2018.08.005.

Cerebral tract integrity relates to white matter hyperintensities, cortex volume, and cognition

Stephan Seiler^{a,b,c}, Evan Fletcher^{a,b}, Kinsy Hassan-Ali^{a,b}, Michelle Weinstein^{a,b}, Alexa Beiser^{d,e,f}, Jayandra J. Himali^{d,e,f}, Claudia L. Satizabal^{d,e}, Sudha Seshadri^{d,e}, Charles DeCarli^{a,b}, and Pauline Maillard^{a,b}

^aDepartment of Neurology and Center for Neurosciences, University of California at Davis, 1544 Newton Court, Davis, CA 95616, USA

^bImaging of Dementia and Aging (IDeA) Laboratory, University of California at Davis, 1544 Newton Court, Davis, CA 95616, USA

^cDepartment of Neurology, Medical University Graz, Auenbruggerplatz 22, 8036 Graz, Austria

^dThe Framingham Heart Study, Framingham, MA, USA

^eDepartment of Neurology, Boston University School of Medicine, 725 Albany St 7B, Boston, MA 02118, USA

^fDepartment of Biostatistics, Boston University School of Public Health, Crosstown Building 801 Massachusetts Avenue, Boston, MA 02118, USA

Abstract

Corresponding author: Stephan Seiler, MD, PhD, Imaging of Dementia & Aging (IDeA) Laboratory, Department of Neurology and Center for Neuroscience, University of California at Davis, 1544 Newton Court, Davis, CA 95616, TEL:(530)-551-9111, FAX: (530)-757-8827, sseiler@ucdavis.edu.

Publisher's Disclaimer: This is a PDF file of an unedited manuscript that has been accepted for publication. As a service to our customers we are providing this early version of the manuscript. The manuscript will undergo copyediting, typesetting, and review of the resulting proof before it is published in its final form. Please note that during the production process errors may be discovered which could affect the content, and all legal disclaimers that apply to the journal pertain.

¹*Abbreviations: WMH=White Matter Hyperintensities, GM=Gray Matter, MRI=Magnetic Resonance Imaging, DTI=Diffusion Tensor Imaging, WM=White Matter, PLS=Partial Least Squares, FA=Fractional Anisotropy, FHS=Framingham Heart Study, LM= Logical Memory Immediate and Delayed recall, PAS= Paired-Associate Memory Immediate and Delayed recall, VR= Visual Reproductions Immediate and Delayed recall, TrA=Trail Making Test A, TrB=Trail Making Test B, TCV=Total Cranial Volume, FLAIR=Fluid-Attenuated Inversion Recovery, CGC=cingulate gyrus part of cingulum, CGH=parahippocampal part of cingulum, FMA=forceps major, FMI=forceps minor, IFO=inferior fronto-occipital fasciculus, ILF=inferior longitudinal fasciculus, PTR=posterior thalamic radiation, TR=Repetition Time, TI=Inversion Time, TE=Echo Time, FOV=Field-Of-View*

6. Disclosure statement

Dr. Seiler reports no disclosures

Dr. Fletcher reports no disclosures

Ms. Hassan-Ali reports no disclosures

Ms. Weinstein reports no disclosures

Dr. Beiser reports no disclosures

Dr. Himali reports no disclosures

Dr. Satizabal reports no disclosures

Dr. Seshadri reports no disclosures

Dr. DeCarli is a consultant to Novartis Pharmaceuticals.

Dr. Maillard reports no disclosures

We examined the relationship between white matter (WM) tract integrity, white matter hyperintensities (WMH), lobar gray matter (GM) volumes and cognition in the cross-sectional Framingham Offspring Study. 680 participants (71.7 ± 7.7 years) completed cognitive testing and MRI. Diffusion tensor imaging (DTI) probabilistic tractography was used to reconstruct major WM tracts. We computed tract-specific mean fractional anisotropy (FA) and tract-specific WMH ratio. Linear regressions identified relations between tracts and lobar GM volumes. Partial least squares regression examined associations between integrity of combined tracts, lobar GM volumes and cognition, including scores of memory and processing speed. Five tracts were particularly vulnerable to WMH and tract-specific WMH volumes were inversely associated with tract-specific FA (p values < 0.05). Tract-specific FA related to lobar GM volumes. Memory was associated with lobar GM, while processing speed related to both tract integrity and lobar GM volumes. We conclude that subtle microstructural WM tract degeneration relates to specific lobar GM atrophy. The integrity of associated WM tracts and GM lobes differentially impacts memory and processing speed.

Keywords

White Matter Hyperintensities; WMH; Cognitive Aging; Magnetic Resonance Imaging; Diffusion Tensor Imaging; Tractography

1. Introduction

Aging is associated with changes in brain structure (DeCarli et al., 2005b) and varying trajectories of cognitive performance (Wilson et al., 2000) including transition to dementia. Changes in brain structure include gray matter (GM) atrophy, subtle white matter (WM) degeneration as reflected by diffusion tensor imaging (DTI) and white matter hyperintensities (WMH) (DeBette et al., 2010). DTI finds that microstructural WM injury in association with vascular risk factors may be present as early as middle age (Maillard et al., 2012) and precede development of WMH (de Groot et al., 2013a; Maillard et al., 2014). While significant relationships between global measures of microstructural WM integrity and WMH (de Groot et al., 2013a; Maillard et al., 2011; Maillard et al., 2014) have been reported, the potential specificity of WM tract vulnerability to WMH and its impact on GM structures remains unclear. Individual WM tracts can be identified by DTI-based probabilistic tractography (de Groot et al., 2013b). Previous studies reported significant associations between tract-specific WM injury, age and vascular risk (de Groot et al., 2015). Tract-specific WM integrity related to worse cognitive performance (Cremers et al., 2016) and higher risk of mortality (Sedaghat et al., 2016). If this happens through disconnection of associated GM structures remains unclear (Friston, 1998) (Duering et al., 2012; Duering et al., 2015). Knowledge about the impact of localized vascular damage, either alone or in combination with neurodegeneration, on cognitive function in normal aging therefore remains limited.

Using probabilistic tractography, we aimed to characterize the specific vulnerability of major WM tracts to WMH development, investigated the relationship between the integrity of WM tracts and that of lobar GM volumes and examined the relationship between integrity of

associated WM tracts and GM lobes and cognitive performance (He et al., 2012) in individuals from the Offspring community-based cohort of the Framingham Heart Study (FHS).

2. Methods

2.1 Study population

The design of the FHS Offspring cohort studies has been detailed previously (Splansky et al., 2007). A total of 752 community-dwelling, cognitively healthy subjects underwent both structural brain MRI and DTI between 2009 and 2014. All subjects at assessment number 9 were given the option to receive an MRI. As previously described (Massaro et al., 2004), all subjects who agreed to have MRI and were not excluded for health reasons were included in this analysis. Participants with prevalent stroke or dementia at the MRI evaluation, however, were excluded from the present analysis (55 participants). Briefly, stroke was defined as an acute onset focal neurologic deficit of presumed vascular etiology, lasting ≥ 24 hours or resulting in death. Dementia was diagnosed according to the criteria of the *DSM-IV* (First et al., 1997). Participants were also excluded from the present analysis for the following reasons: other neurologic disorders that might confound the assessment of brain volumes, or poor brain MRI quality (17 participants), resulting in a final sample of 680 individuals. Demographic characteristics are summarized in Table 1.

2.2 Standard protocol approvals, registrations, and patient consents

The Institutional Review Boards at all participating institutions approved this study, and subjects or their legal representatives gave written informed consent.

2.3 Cognitive outcomes

We used three memory summary scores from the Wechsler Memory Scale (Wechsler, 1945), derived by factor analysis from the larger FHS-cognitive battery (Au et al., 2004; Downer et al., 2015). All three summary scores showed high capability in differentiating between normal, multi-domain impaired, and dementia participants (Downer et al., 2015). In brief, the tests assess verbal memory (Logical Memory Immediate and Delayed recall [LM]), learning (Paired-Associate Memory Immediate and Delayed recall [PAS]), and visual memory (Visual Reproductions Immediate and Delayed recall [VR]). Two tests assessed visual-motor skills, set switching and processing speed (Trail Making Test A and B [TrA and TrB](Armitage, 1946)). For tests with immediate and delayed scores, the average of the two scores was computed and used as the outcome measure. TrA and TrB are timed assessments that require a participant to connect a random alphabetic sequence (TrA) and alphanumeric sequence (TrB). TrA and TrB measures were log-transformed to normalize population variance, and multiplied by -1 to harmonize directionality of effects among subtests. For each test, except for TrA and TrB, a higher score indicates better cognitive function.

2.4 Image acquisition and processing

Participants were evaluated with a 1.5-Tesla Siemens Avanto scanner. Three sequences were used: 3-dimensional T1-weighted coronal spoiled gradient-recalled echo (SPGR)

acquisition (repetition time (TR)=1900ms, echo time (TE)=2.96ms, inversion time (TI)=1100ms, 1,5mm isotropic resolution), fluid attenuated inversion recovery (FLAIR) sequence (TR=9000ms, TE=123ms, TI=2500ms, in-plane resolution 0.86×0.86mm, slice thickness 3mm), and diffusion tensor imaging (DTI). A DTI sequence suitable for fiber tractography (Mukherjee et al., 2008) was performed using the following parameters: TR=3600 ms, TE=94 ms, 25 contiguous slices total, with no gaps between sections, field-of-view (FOV)=25 cm, acquisition matrix = 128 × 128, slice thickness = 5 mm. Acquisition was interleaved to prevent cross-talk between adjacent contiguous sections. Diffusion weighted images were generated using 30 gradient directions, repeated four times, with total gradient diffusion sensitivity of $b = 1000 \text{ s/mm}^2$, and four unweighted images with $b = 0 \text{ s/mm}^2$.

Centralized reading of all images was performed using in-house designed imaging, visualization and analysis software (Quanta 2) (DeCarli et al., 2005a). Segmentation of GM was performed on native T1-weighted images using an in-house implementation of a Bayesian maximum-likelihood expectation-maximization algorithm method (Dempster et al., 1977). Lobar GM volumes and total cranial volume (TCV) were quantified using previously reported analysis protocols (Lee et al., 2010). TCV was used to correct for differences in head size (DeCarli et al., 2005a). Tractography was performed using FSL tools (Jenkinson et al., 2012) including PROBTRACKX (Behrens et al., 2007), a Bayesian approach to probabilistic tractography, and AutoPTX (de Groot et al., 2015), a protocol for identifying major white matter tracts (de Groot et al., 2013b). Tractography and computation of fractional anisotropy (FA) was performed for each subject in the subject's DTI image native space, after transformation of voxels' dimension to isotropic (i.e., section thickness is the same as the inplane pixel length). For the present study, we used tracts that could be robustly identified (Mori et al., 2002; Wakana et al., 2004), including the cingulate gyrus part of cingulum (CGC), parahippocampal part of cingulum (CGH), forceps major (FMA), forceps minor (FMI), inferior fronto-occipital fasciculus (IFO), inferior longitudinal fasciculus (ILF), uncinate (UNC), superior longitudinal fasciculus (SLF), corticospinal tract (CST), superior thalamic radiation (STR), anterior thalamic radiation (ATR), acoustic radiation (ACR) and posterior thalamic radiation (PTR). The resulting tract-density (visitation count) images for each tract were normalized by division with the total number of particles (tracts) in the tractography run and thresholded (de Groot et al., 2015).

The segmentation of WMH was performed using a semi-automated procedure that has been previously described (DeCarli et al., 2005a) and which demonstrates high inter-rater reliability (Carmichael et al., 2010). For each individual, the subject's FLAIR image was linearly coregistered into the subject's DTI space, and resulting transformation parameters applied to the subject's WMH map.

2.5 Tract-derived measures

For each subject and each tract, mean FA was computed by superimposing the thresholded tract map to the subject's FA image and included voxels from the normal appearing WM (NAWM) and WMH voxels. Tract-specific total volume was defined as the number of voxels within the tract multiplied by the image voxel size. Tract-specific WMH volumes were

computed by superimposing, for each subject individually, the WMH map onto tract images, and by multiplying WMH voxels within the tract by the image voxel size. Tract-specific WMH ratio was calculated by dividing tract-specific WMH volume by the corresponding tract total volume. Tract-specific WMH ratios were log-transformed to normalize population variance.

2.6 Statistical analysis

To identify tracts of interest, we screened the 13 original tracts for univariate correlations with cognition (linear regression with tract-based mean FA as independent and cognitive test scores as dependent variables, adjusted for age, sex and education). Those 9 tracts that showed at least one significant correlation ($p < 0.05$) with a cognitive test score were included in further analyses (supplementary table 1). Tract-specific WMH ratios of 9 tracts of interest can be seen in Table 2 and Fig. 1.

For visualization purpose only, individuals' WM tract and WMH maps were coregistered to a DTI template available in FSL (Jenkinson et al., 2012) (FMRIB58_FA template). Frequency maps were generated and thresholded (20%), resulting in a composite image of WM tracts as illustrated in Fig.2.

MRI variables, including tract-specific FA, tract-specific WMH ratio (log-transformed), lobar GM volumes, and cognitive measures, including scores in LM, VR, PAS, TrA and TrB, were first regressed against age, gender, systolic blood pressure, fasting blood glucose, education level and TCV using linear regressions. Resulting residuals were used in all analyses described below.

The first objective of the study was to characterize the potential tract-specific vulnerability to WMH. To address this goal, we used a linear mixed-effects model to investigate whether WM tracts were differentially subject to WMH development and whether FA may play a role in this tract-specific vulnerability. Regression included tract-specific WMH ratio as the dependent variable, tract-specific FA and tract label as independent variables and random effects due to subject's identity. In a complementary analysis, we repeated this regression using tract-specific FA computed within voxels from the NAWM only (i.e. not including WMH voxels). The results did not change substantially (see Supplementary Table 2).

The second goal of the study was to investigate the relationships between tract-specific FA and WMH ratio separately with regional GM volumes. To assess this goal, we used linear regressions with lobar GM volumes, which have been reported to strongly and independently correlate with cognition in one of our recent studies (Fletcher et al., 2018). GM volumes were segmented and served as separate dependent variables and either tract-specific FA or WMH ratio as independent variables.

Results were corrected for multiple comparisons using Bonferroni correction. Because localized and global brain injuries are strongly correlated, we included overall mean FA or overall WMH burden (log-transformed) as additional covariates (table 3).

Finally, we investigated the associations between cognitive performance, including scores in LM, VR, PAS, TrA and TrB, and the integrity of WM tracts and GM lobes that were found

significantly associated using partial least squares regression (PLSR). PLSR searches for a set of components that perform a simultaneous decomposition of X (i.e. combination of neural measures) and Y (cognitive performance) with the constraint that these components explain as much as possible of the covariance between X and Y. In the present study, we performed a PLSR regression for each of the four combinations of neural measures (each GM lobar volume along with the corresponding associated WM tracts) and each of the five cognitive tests. Our analyses aim to investigate two things: first, which combination of neural measures accounts for more variance in each test performance (assessed by the R^2); and second, within this combination, the implication of each of the neural measures, in term of load size. Resulting p-values were corrected for multiple comparisons using Bonferroni correction. Statistical analyses were performed using R version 3.0.2 (R Development Core Team, 2013, Vienna, Austria).

3. Results

3.1 Tract-specific vulnerability to WMH

Distribution of WMH ratios and mean FA values across tracts are reported in Table 2 and are illustrated in Figs. 1 and 3. WMH ratios were differently distributed across tracts. 5 tracts were particularly prone to WMH occurrence. FMA was most affected (mean \pm SD WMH ratio: 3.94 \pm 4.57%), followed by PTR (2.85 \pm 3.92%), IFO (2.09 \pm 3.31%), FMI (1.94 \pm 2.75%), and ILF (1.84 \pm 2.82%). Fig. 4 shows the spatial distribution at voxel level of WMH ratio within these tracts across the study sample.

Logistic regression revealed a significant effect of tract label ($\chi^2=2665.55$, $p<0.001$), indicating that WMH ratios were significantly different across tracts, and of mean FA ($\chi^2=3.88$, $p=0.049$), indicating that decreased FA was significantly associated with increased WMH ratio. The model also indicated a significant interaction between the two variables ($\chi^2=942.87$, $p<0.001$). *Post hoc* analyses revealed that decrease in FA was associated with higher risk of WMH occurrence for all tracts (table 2). Logistic regression curves for the relationships between tract-specific WMH ratios on tract-specific mean FA are illustrated in Fig. 5.

3.2 Associations of tract-specific FA and WMH with lobar GM volumes

Frontal lobe gray matter volume was found to be associated with CGH FA ($\beta=0.16$, $p<0.05$), FMA FA ($\beta=0.15$, $p<0.05$) and FMI FA ($\beta=0.25$, $p<0.001$). Occipital lobe gray matter volume was found to be associated with CGC FA ($\beta=-0.15$, $p<0.01$), FMA FA ($\beta=0.25$, $p<0.001$), FMI FA ($\beta=0.18$, $p<0.01$) and PTR FA ($\beta=0.17$, $p<0.01$). Parietal lobe gray matter volume was found to be associated with CGH FA ($\beta=0.14$, $p<0.05$) and FMI FA ($\beta=0.20$, $p<0.001$) and temporal lobe gray matter volume with CHG FA ($\beta=0.23$, $p<0.001$), FMA FA ($\beta=0.20$, $p<0.001$) and UNC FA ($\beta=0.20$, $p<0.001$).

FMA WMH were significantly associated with occipital GM volume only ($\beta =-0.22$, $p<0.01$) (table 3).

3.3 Relationship of integrity of associated tract-specific FA and lobar GM with cognitive performances

PLS regressions were performed to investigate the association between scores in LM, VR, PAS, TrA and TrB, tract-specific FA, and lobar GM volumes that were found to be associated with these tracts (frontal lobe with CGH, FMA and FMI, occipital lobe with CGC, FMA, FMI and PTR, parietal lobe with CGH and FMI, and temporal lobe with CGH, FMA, and UNC). Scores on tests of memory function were found to be associated with the combination of temporal lobe gray matter volume with CGH, FMA, and UNC FA (LM: $R^2=0.018, p<0.05$, VR: $R^2=0.038, p<0.001$, PAS: $R^2=0.021, p<0.01$), combination of parietal lobe gray matter volume with CGH and FMI FA (VR: $R^2=0.035, p<0.001$ and PAS: $R^2=0.017, p<0.05$) and combination of frontal lobe gray matter volume with CGH, FMA and FMI FA (VR: $R^2=0.028, p<0.001$). Standardized component coefficients associated with these associations mostly implicated lobar GM volumes (Table 4).

Scores on tests of information processing speed were found to be associated with combination of temporal lobe gray matter volume with CGH, FMA and UNC FA (TrA: $R^2=0.053, p<0.001$; TrB: $R^2=0.049, p<0.001$), combination of occipital lobe gray matter volume with CGC, FMA, FMI and PTR FA (TrA: $R^2=0.052, p<0.001$; TrB: $R^2=0.028, p<0.001$), combination of frontal lobe gray matter volume with CGH, FMA and FMI FA (TrA: $R^2=0.047, p<0.001$; TrB: $R^2=0.036, p<0.001$) and combination of parietal lobe gray matter volume with CGH and FMI FA (TrA: $R^2=0.039, p<0.001$; TrB: $R^2=0.035, p<0.001$). Standardized component coefficients associated with these associations were balanced between tract-specific FA and lobar GM volumes (Table 4), except for the association between TrA and combination of frontal lobe gray matter with CGH, FMA and FMI FA that indicated a predominant role of tract integrity measures as opposed to frontal GM (0.088, 0.100 and 0.084 vs. 0.012).

4. Discussion

Our study has three major findings. First, specific WM tracts are particularly vulnerable to WMH occurrence, including the posterior thalamic radiation, the forceps minor and major and the inferior fronto-occipital and longitudinal fasciculi. Second, tract-specific integrity, as expressed with FA, is associated with specific lobar GM volumes.

Third, performance on test of memory are mostly associated with integrity of lobar GM, while performance on tests of information processing speed are associated with both integrity of white matter tracts and lobar GM volumes. We discuss the significance of each finding in turn.

4.1 Spatial distribution of WMH among tracts

Recent studies suggest that WMH volumes in individual tracts explain more variance in cognition than total WMH burden, emphasizing the importance of lesion location when addressing the functional consequences of WMH (Biesbroek et al., 2016). It is therefore important to characterize age-related vulnerability of specific tracts to WMH in the cognitively normal population, which, so far, has received limited investigation. The present

study suggests that WMH impact WM tracts differently in the older population within the posterior thalamic radiation, the forceps minor and major as well as two major association tracts, including the inferior fronto-occipital and longitudinal fasciculi, being particularly susceptible to WMH development, confirming recent findings from the Rotterdam study (Langen et al., 2017). Conversely, some tracts, including the cingulum, the superior longitudinal fasciculus and the uncinate, do not appear to be particularly vulnerable to WMH development. There are two potential hypotheses to explain such localized specificity in WMH development. First, it may be explained by the intrinsic organization of the underlying WM tracts (Lee et al., 2009). Indeed, WM tracts are composed of fibers that are different in terms of number and diameter (Mori and van Zijl, 2002); and while the present study, as others (Langen et al., 2017), found that integrity of all WM tracts decreases with age (data not shown), such specific-tract properties may impact the delay by which more severe injury, as expressed by WMH, occurs. Second, WMH development may be higher within tracts that belong to vascular territories. Indeed, it has been reported that occurrence of WMH is particularly high in the WM periventricular watershed areas (Duering et al., 2013), but also in WM regions with increased free water content (Maillard et al., 2017) which may be more specific to the watershed of the middle cerebral artery circulation. Recent studies on brain aging combining DTI and FLAIR imaging suggest that WM degeneration is a continuous process over time with subtle changes in WM integrity, as reflected with FA, that ultimately lead to WMH (de Groot et al., 2013a; Maillard et al., 2014). On tract-level, the relationship between WM integrity and WMH has been less well documented. The present study suggests that, in a community-dwelling population of healthy adults, microstructural integrity of specific tracts is associated with WMH burden within the corresponding tract. With regards to accumulating evidence that microstructural WM changes, that can occur as early as the fourth decade in life, precede WMH development in the overall WM (de Groot et al., 2013a; Maillard et al., 2014), our result suggests that, in specific tracts, subtle WM degeneration may lead to greater localized WMH. This notion is further supported by our finding that correlations between tract-wise average FA and tract-wise FA in NAWM with tract-specific WMH were of similar magnitude and direction. Longitudinal studies are needed to confirm the direction of causality for these associations.

4.2 Relationship of tract-specific FA with adjacent GM volumes

The brain white matter consists primarily of myelinated axons that form the anatomic connections between various brain regions resulting in specific functional networks (Waxman et al., 1995). Major efforts have been deployed to understand brain intrinsic networks through functional connectivity studies (Huettel, 2009). Yet, despite overwhelming evidence that activities in different GM regions are dependent upon the microstructural organization of the axons connecting them (Greicius et al., 2009; Langen et al., 2017), characterizing structural connectivity, in terms of integrity and physiology, of WM tracts and GM terminals connected to the tracts has received limited attention, especially among cognitively normal individuals. It has been reported that fiber tracts FA correlated inversely with cerebral blood flow, and the GM terminals connected to the tract also tended to have a lower temporal synchrony in resting-state BOLD signal fluctuation (Aslan et al., 2011). It has also been reported that incident lacunar infarcts, which occur preferentially in the

vicinity of WMH (Duering et al., 2013), are related to adjacent cortical thinning through microstructural damage of connected WM tracts (Duering et al., 2012; Duering et al., 2015). The present study extends these findings by showing that subtle WM injury, as expressed by FA in specific tracts also relates to specific lobar GM volumes. Larger frontal GM volume was found to be associated with higher FA within the FMI and FMA. Association with FMI is biologically relevant, as FMI constitutes a fiber bundle that connects bilateral frontal cortices via the genu of the corpus callosum. One hypothesis to explain the correlation between frontal GM and the FMA may be that neuronal networks communicate across other, more subtle tracts not included in the present study, which focused mainly on major WM tracts. In this context, one recent study on tract-based WMH and functional connectivity between specific cortex regions is of note. The authors found that tract-specific WMH within specific tracts altered functional connectivity between cortex regions that were connected by other, different tracts, which were even less affected by WMH (Langen et al., 2017). The uncinate fasciculus and the hippocampal part of the cingulum correlated strongly with temporal lobe GM, in accordance with their anatomical localization (Jones et al., 2013; Wakana et al., 2004). A weaker correlation between parietal lobe volume and CGH might be due to smaller tracts that are not represented in our study, including subtle temporo-parietal connections (Szczepanski and Saalman, 2013). Indirect connections that elude our analysis might be better amenable to structural connectome analysis, performed on high-resolution DTI data, which allows identification of much subtler direct- and indirect connections (Sporns, 2013). We accounted for a possible unspecific confounding effect of global FA on GM volume by including global FA as covariate in our analysis, but indirect relationships remained significant. It is therefore possible that other factors, like AD pathology or vascular risk, mediate some of the indirect relationships. Tract-specific WMH burden was not found to substantially impact lobar GM volume. One potential explanation resides in that, as described above, WMH are the extreme expression of more general injury (Maillard et al., 2011), but subtle vascular injury, as evidenced with reduced FA, has been reported to start as early as the fourth decade (Maillard et al., 2012), and its cumulative deleterious impact, over time, on GM volume may reach a stage that, when WMH finally emerge, is already too advanced.

4.3 Association between integrity of associated WM tracts and GM lobes and cognitive performance

Variance in memory scores was found to be explained by lobar GM volume rather than tract-specific FA. Associations mostly implicated parietal and temporal GM atrophy. Volume loss of parieto-temporal GM is a hallmark of AD and has been reported to be detectable even in healthy adults at risk for the disease (Dickerson et al., 2012) (Smith et al., 2007). Parieto-temporal GM atrophy has also been found to identify cognitively healthy individuals at risk for future memory decline (Chiang et al., 2011) and MCI (Smith et al., 2007). Consistent with prior studies, which reported weak associations between WM tracts integrity and memory performance (Cremers et al., 2016), we also found largely weaker associations as compared to those with lobar gray matter volumes. One hypothesis is that GM volume is more sensitive to individual differences in memory performance than FA from the assessed tracts, because tracts that are more involved in memory processing were not extensively studied. Because of limitations of the FSL-tool used, we could not include the fornix, where

neurodegeneration-related tract effects may be greater (Ezzati et al., 2016). In this context, however, one of our recent studies is of interest. We found that fornix microstructure related to memory performance, but not independent of hippocampus volume (Lee et al., 2012). A similar overshadowing effect of volume over connected white matter tracts with respect to memory performance might apply in the present study. We included uncinate and cingulum bundle, which did not show a substantially higher correlation with memory performance, as compared to their connected GM volumes. It remains unclear why lobar volumes in our study are more sensitive to individual differences in memory performance. One explanation could be that other white matter connections, besides the fornix, could be important for memory and were not captured by our analysis.

While the importance of WM tract network integrity to maintain information processing speed is well established (Cremers et al., 2016; Kuznetsova et al., 2016), the understanding of the concomitant role of GM structures, along with that of their associated tracts, remains limited (Tartaglia et al., 2012). In the present study, most GM-tract-combinations identified by our linear regression models correlated more strongly with processing speed than with memory. Within these combinations, we found shared influence of the load sizes of both temporal, parietal and occipital GM volumes and their connected WM tracts on processing speed, in line with the hypothesis of influence of complex relationships between different lobar GM volumes, white matter tracts and scores of executive function including processing speed (Collette et al., 2006; Turken et al., 2008). Interestingly, this finding did not include the combination of frontal GM with its respective associated tracts (FMI, FMA, CGH). Within this combination, the individual load sizes for tract integrity were found to be up to eight times larger than that of frontal GM volume. The FMI and FMA connect frontal-and occipital cortical areas across the midline via the corpus callosum and are important for executive functioning, including processing speed (Duering et al., 2014) (Catani et al., 2003; Sullivan et al., 2006). Our segmentation of the frontal lobe GM volume might be simply too coarse to find correlations with processing speed scores. Future studies might want to avoid this constraint by using finer parcellations of the frontal GM.

4.4 Strengths and limitations

Strengths of our study are the large, population based sample with quantitative and sensitive measurements of WM integrity, thorough vascular risk factor assessments and detailed neuropsychological testing. We combined quantification of tract-specific alterations on a micro-and macrostructural level using modern and publicly available tractography methods (de Groot et al., 2013b), and assessed the relationship between these white matter tract-specific alterations and gray matter volumes, to show their shared influences on processing speed and memory performance while correcting for effects of whole-brain micro-and macrostructural damage, age, and vascular risk factors. There are also limitations. Although the tract segmentation algorithm covers a fairly large number of white matter tracts (de Groot et al., 2013b), there are still other direct-and indirect white matter connections (Sporns, 2013) that are not segmented and therefore elude to our analysis. Future studies might want to use full graph analysis with a finer cortical- and subcortical parcellation to get a more fine-grained picture of the relationships between small cortical regions including hippocampus and thalamus, and more localized WM tracts. Furthermore, the biological

mechanisms by which altered tract microstructure may lead to atrophy of localized GM has to be determined. The present study does not enable to determine whether GM atrophy results from dendritic and cell-body atrophy or from neuronal loss as suggested by a recent study that examined the relationship between cortical neurofibrillary tangle counts and subcortical white matter integrity in the parietal region of individuals suffering with Alzheimer's disease (McAleese et al., 2017). An alternative likely mechanism may be secondary neurodegeneration after the disruption of subcortical axons by vascular injury leading to transected neuronal degeneration as previously shown for lesions of the optic nerve and animal models of axotomy (Siffrin et al., 2010). Future studies will want to include neuroimaging techniques like FDG-PET, Amyloid-PET and tau-PET as well as AD genotyping to identify participants at risk for Alzheimer's disease to more thoroughly identify prevalent Alzheimer's pathology. The cross-sectional design of the present study does not permit conclusions on the chronology and direction of causality, either unilateral or bilateral, of these associations. Further longitudinal studies are needed to clarify these questions. Finally, the FHS cohort is mostly of white descent and therefore does not fully represent the general population of the United States. Replication of our results in an ethnically more diverse cohort would be warranted.

5. Conclusion

The present study finds that subtle microstructural WM tract degeneration is associated with tract-specific injury as reflected by higher WMH load, and with specific lobar GM atrophy. The integrity of associated WM tracts and lobar GM volumes was found to impact differentially episodic memory and information processing speed. These findings are of importance to better understand the impact of located vascular damage, either alone or in combination with neurodegeneration, on cognitive functions in normal aging.

Supplementary Material

Refer to Web version on PubMed Central for supplementary material.

Acknowledgments

7. Funding

The study was supported by NIH/NHLBI contracts P30-AG010129, R01-AG033040, R01-AG08122, K23-LH118529, N01-HC-25195, HHSN268201500001I, HL076784, AG028321, HL070100, HL060040, HL080124, HL071039, HL077447, HL107385, and 2-K24-HL04334.

8. References

- Armitage SG, 1946 An analysis of certain psychological tests used for the evaluation of brain injury. *Psychological Monographs* 60(1), i-48.
- Aslan S, Huang H, Uh J, Mishra V, Xiao G, van Osch MJ, Lu H, 2011 White matter cerebral blood flow is inversely correlated with structural and functional connectivity in the human brain. *Neuroimage* 56(3), 1145-1153. [PubMed: 21385618]
- Au R, Seshadri S, Wolf PA, Elias M, Elias P, Sullivan L, Beiser A, D'Agostino RB, 2004 New norms for a new generation: cognitive performance in the framingham offspring cohort. *Exp Aging Res* 30(4), 333-358. [PubMed: 15371099]

- Behrens TE, Berg HJ, Jbabdi S, Rushworth MF, Woolrich MW, 2007 Probabilistic diffusion tractography with multiple fibre orientations: What can we gain? *Neuroimage* 34(1), 144–155. [PubMed: 17070705]
- Biesbroek JM, Weaver NA, Hilal S, Kuijff HJ, Ikram MK, Xu X, Tan BY, Venketasubramanian N, Postma A, Biessels GJ, Chen CP, 2016 Impact of Strategically Located White Matter Hyperintensities on Cognition in Memory Clinic Patients with Small Vessel Disease. *PLoS One* 11(11), e0166261. [PubMed: 27824925]
- Carmichael O, Mungas D, Beckett L, Harvey D, Tomaszewski Farias S, Reed B, Olichney J, Miller J, Decarli C, 2010 MRI predictors of cognitive change in a diverse and carefully characterized elderly population. *Neurobiol Aging*.
- Catani M, Jones DK, Donato R, Ffytche DH, 2003 Occipito-temporal connections in the human brain. *Brain* 126(Pt 9), 2093–2107. [PubMed: 12821517]
- Chiang GC, Insel PS, Tosun D, Schuff N, Truran-Sacrey D, Raptentsetsang S, Jack CR, Weiner MW, Initiative, A.s.D.N., 2011 Identifying cognitively healthy elderly individuals with subsequent memory decline by using automated MR temporoparietal volumes. *Radiology* 259(3), 844–851. [PubMed: 21467255]
- Collette F, Hogge M, Salmon E, Van der Linden M, 2006 Exploration of the neural substrates of executive functioning by functional neuroimaging. *Neuroscience* 139(1), 209–221. [PubMed: 16324796]
- Cremers LG, de Groot M, Hofman A, Krestin GP, van der Lugt A, Niessen WJ, Vernooij MW, Ikram MA, 2016 Altered tract-specific white matter microstructure is related to poorer cognitive performance: The Rotterdam Study. *Neurobiol Aging* 39, 108–117. [PubMed: 26923407]
- de Groot M, Ikram MA, Akoudad S, Krestin GP, Hofman A, van der Lugt A, Niessen WJ, Vernooij MW, 2015 Tract-specific white matter degeneration in aging: the Rotterdam Study. *Alzheimers Dement* 11(3), 321–330. [PubMed: 25217294]
- de Groot M, Verhaaren BF, de Boer R, Klein S, Hofman A, van der Lugt A, Ikram MA, Niessen WJ, Vernooij MW, 2013a Changes in normal-appearing white matter precede development of white matter lesions. *Stroke* 44(4), 1037–1042. [PubMed: 23429507]
- de Groot M, Vernooij MW, Klein S, Ikram MA, Vos FM, Smith SM, Niessen WJ, Andersson JL, 2013b Improving alignment in Tract-based spatial statistics: evaluation and optimization of image registration. *Neuroimage* 76, 400–411. [PubMed: 23523807]
- Debette S, Beiser A, DeCarli C, Au R, Himali JJ, Kelly-Hayes M, Romero JR, Kase CS, Wolf PA, Seshadri S, 2010 Association of MRI markers of vascular brain injury with incident stroke, mild cognitive impairment, dementia, and mortality: the Framingham Offspring Study. *Stroke* 41(4), 600–606. [PubMed: 20167919]
- DeCarli C, Fletcher E, Ramey V, Harvey D, Jagust WJ, 2005a Anatomical mapping of white matter hyperintensities (WMH): exploring the relationships between periventricular WMH, deep WMH, and total WMH burden. *Stroke* 36(1), 50–55. [PubMed: 15576652]
- DeCarli C, Massaro J, Harvey D, Hald J, Tullberg M, Au R, Beiser A, D'Agostino R, Wolf PA, 2005b Measures of brain morphology and infarction in the framingham heart study: establishing what is normal. *Neurobiol Aging* 26(4), 491–510. [PubMed: 15653178]
- Dempster AP, Laird NM, Rubin DB, 1977 Maximum Likelihood from Incomplete Data Via Em Algorithm. *J Roy Stat Soc B Met* 39(1), 1–38.
- Dickerson BC, Wolk DA, Initiative, A.s.D.N., 2012 MRI cortical thickness biomarker predicts AD-like CSF and cognitive decline in normal adults. *Neurology* 78(2), 84–90. [PubMed: 22189451]
- Downer B, Fardo DW, Schmitt FA, 2015 A Summary Score for the Framingham Heart Study Neuropsychological Battery. *J Aging Health* 27(7), 1199–1222. [PubMed: 25804903]
- Duering M, Csanadi E, Gesierich B, Jouvent E, Hervé D, Seiler S, Belaroussi B, Ropele S, Schmidt R, Chabriat H, Dichgans M, 2013 Incident lacunes preferentially localize to the edge of white matter hyperintensities: insights into the pathophysiology of cerebral small vessel disease. *Brain* 136(Pt 9), 2717–2726. [PubMed: 23864274]
- Duering M, Gesierich B, Seiler S, Pirpamer L, Gonik M, Hofer E, Jouvent E, Duchesnay E, Chabriat H, Ropele S, Schmidt R, Dichgans M, 2014 Strategic white matter tracts for processing speed deficits in age-related small vessel disease. *Neurology* 82(22), 1946–1950. [PubMed: 24793184]

- Duering M, Righart R, Csanadi E, Jouvent E, Hervé D, Chabriat H, Dichgans M, 2012 Incident subcortical infarcts induce focal thinning in connected cortical regions. *Neurology* 79(20), 2025–2028. [PubMed: 23054230]
- Duering M, Righart R, Wollenweber FA, Zietemann V, Gesierich B, Dichgans M, 2015 Acute infarcts cause focal thinning in remote cortex via degeneration of connecting fiber tracts. *Neurology* 84(16), 1685–1692. [PubMed: 25809303]
- Ezzati A, Katz MJ, Lipton ML, Zimmerman ME, Lipton RB, 2016 Hippocampal volume and cingulum bundle fractional anisotropy are independently associated with verbal memory in older adults. *Brain Imaging Behav* 10(3), 652–659. [PubMed: 26424564]
- First MB, Spitzer RL, Gibbon M, Williams JBW, 1997 Structured Clinical Interview for DSM-IV Axis I Disorders (SCID-I), Clinical Version. American Psychiatric Press, Inc., Washington, DC.
- Fletcher E, Gavett B, Harvey D, Farias ST, Olichney J, Beckett L, DeCarli C, Mungas D, 2018 Brain volume change and cognitive trajectories in aging. *Neuropsychology*.
- Friston KJ, 1998 The disconnection hypothesis. *Schizophr Res* 30(2), 115–125. [PubMed: 9549774]
- Greicius MD, Supekar K, Menon V, Dougherty RF, 2009 Resting-state functional connectivity reflects structural connectivity in the default mode network. *Cereb Cortex* 19(1), 72–78. [PubMed: 18403396]
- He J, Wong VS, Fletcher E, Maillard P, Lee DY, Iosif AM, Singh B, Martinez O, Roach AE, Lockhart SN, Beckett L, Mungas D, Farias ST, Carmichael O, DeCarli C, 2012 The contributions of MRI-based measures of gray matter, white matter hyperintensity, and white matter integrity to late-life cognition. *AJNR Am J Neuroradiol* 33(9), 1797–1803. [PubMed: 22538073]
- Huettel SA, Song AW, McCarthy G, 2009 Functional magnetic resonance imaging. Sinauer Associates, Sunderland, Mass.
- Jenkinson M, Beckmann CF, Behrens TE, Woolrich MW, Smith SM, 2012 FSL. *Neuroimage* 62(2), 782–790. [PubMed: 21979382]
- Jones DK, Christiansen KF, Chapman RJ, Aggleton JP, 2013 Distinct subdivisions of the cingulum bundle revealed by diffusion MRI fibre tracking: implications for neuropsychological investigations. *Neuropsychologia* 51(1), 67–78. [PubMed: 23178227]
- Kuznetsova KA, Maniega SM, Ritchie SJ, Cox SR, Storkey AJ, Starr JM, Wardlaw JM, Deary IJ, Bastin ME, 2016 Brain white matter structure and information processing speed in healthy older age. *Brain Struct Funct* 221(6), 3223–3235. [PubMed: 26254904]
- Langen CD, Zonneveld HI, White T, Huizinga W, Cremers LG, de Groot M, Ikram MA, Niessen WJ, Vernooij MW, 2017 White matter lesions relate to tract-specific reductions in functional connectivity. *Neurobiol Aging* 51, 97–103. [PubMed: 28063366]
- Lee DY, Fletcher E, Carmichael OT, Singh B, Mungas D, Reed B, Martinez O, Buonocore MH, Persianinova M, DeCarli C, 2012 Sub-Regional Hippocampal Injury is Associated with Fornix Degeneration in Alzheimer's Disease. *Front Aging Neurosci* 4, 1. [PubMed: 22514534]
- Lee DY, Fletcher E, Martinez O, Ortega M, Zozulya N, Kim J, Tran J, Buonocore M, Carmichael O, DeCarli C, 2009 Regional pattern of white matter microstructural changes in normal aging, MCI, and AD. *Neurology* 73(21), 1722–1728. [PubMed: 19846830]
- Lee DY, Fletcher E, Martinez O, Zozulya N, Kim J, Tran J, Buonocore M, Carmichael O, DeCarli C, 2010 Vascular and degenerative processes differentially affect regional interhemispheric connections in normal aging, mild cognitive impairment, and Alzheimer disease. *Stroke* 41(8), 1791–1797. [PubMed: 20595668]
- Maillard P, Fletcher E, Harvey D, Carmichael O, Reed B, Mungas D, DeCarli C, 2011 White matter hyperintensity penumbra. *Stroke* 42(7), 1917–1922. [PubMed: 21636811]
- Maillard P, Fletcher E, Lockhart SN, Roach AE, Reed B, Mungas D, DeCarli C, Carmichael OT, 2014 White matter hyperintensities and their penumbra lie along a continuum of injury in the aging brain. *Stroke* 45(6), 1721–1726. [PubMed: 24781079]
- Maillard P, Mitchell GF, Himali JJ, Beiser A, Fletcher E, Tsao CW, Pase MP, Satizabal CL, Vasan RS, Seshadri S, DeCarli C, 2017 Aortic Stiffness, Increased White Matter Free Water, and Altered Microstructural Integrity: A Continuum of Injury. *Stroke*.
- Maillard P, Seshadri S, Beiser A, Himali JJ, Au R, Fletcher E, Carmichael O, Wolf PA, DeCarli C, 2012 Effects of systolic blood pressure on white-matter integrity in young adults in the

- Framingham Heart Study: a cross-sectional study. *Lancet Neurol* 11(12), 1039–1047. [PubMed: 23122892]
- Massaro JM, D'Agostino RB, Sr., Sullivan LM, Beiser A, DeCarli C, Au R, Elias MF, Wolf PA, 2004 Managing and analysing data from a large-scale study on Framingham Offspring relating brain structure to cognitive function. *Stat Med* 23(2), 351–367. [PubMed: 14716734]
- McAleese KE, Walker L, Graham S, Moya ELJ, Johnson M, Erskine D, Colloby SJ, Dey M, Martin-Ruiz C, Taylor JP, Thomas AJ, McKeith IG, De Carli C, Attems J, 2017 Parietal white matter lesions in Alzheimer's disease are associated with cortical neurodegenerative pathology, but not with small vessel disease. *Acta Neuropathol.*
- Mori S, Kaufmann WE, Davatzikos C, Stieltjes B, Amodei L, Fredericksen K, Pearlson GD, Melhem ER, Solaiyappan M, Raymond GV, Moser HW, van Zijl PC, 2002 Imaging cortical association tracts in the human brain using diffusion-tensor-based axonal tracking. *Magn Reson Med* 47(2), 215–223. [PubMed: 11810663]
- Mori S, van Zijl PC, 2002 Fiber tracking: principles and strategies - a technical review. *NMR Biomed* 15(7-8), 468–480. [PubMed: 12489096]
- Mukherjee P, Chung SW, Berman JI, Hess CP, Henry RG, 2008 Diffusion tensor MR imaging and fiber tractography: technical considerations. *AJNR Am J Neuroradiol* 29(5), 843–852. [PubMed: 18339719]
- Sedaghat S, Cremers LG, de Groot M, Hofman A, van der Lugt A, Niessen WJ, Franco OH, Dehghan A, Ikram MA, Vernooij MW, 2016 Lower microstructural integrity of brain white matter is related to higher mortality. *Neurology* 87(9), 927–934. [PubMed: 27488598]
- Siffrin V, Vogt J, Radbruch H, Nitsch R, Zipp F, 2010 Multiple sclerosis - candidate mechanisms underlying CNS atrophy. *Trends Neurosci* 33(4), 202–210. [PubMed: 20153532]
- Smith CD, Chebrolu H, Wekstein DR, Schmitt FA, Jicha GA, Cooper G, Markesbery WR, 2007 Brain structural alterations before mild cognitive impairment. *Neurology* 68(16), 1268–1273. [PubMed: 17438217]
- Splansky GL, Corey D, Yang Q, Atwood LD, Cupples LA, Benjamin EJ, D'Agostino RB, Sr., Fox CS, Larson MG, Murabito JM, O'Donnell CJ, Vasan RS, Wolf PA, Levy D, 2007 The Third Generation Cohort of the National Heart, Lung, and Blood Institute's Framingham Heart Study: design, recruitment, and initial examination. *Am J Epidemiol* 165(11), 1328–1335. [PubMed: 17372189]
- Sporns O, 2013 The human connectome: origins and challenges. *Neuroimage* 80, 53–61. [PubMed: 23528922]
- Sullivan EV, Adalsteinsson E, Pfefferbaum A, 2006 Selective age-related degradation of anterior callosal fiber bundles quantified in vivo with fiber tracking. *Cereb Cortex* 16(7), 1030–1039. [PubMed: 16207932]
- Szczepanski SM, Saalman YB, 2013 Human fronto-parietal and parieto-hippocampal pathways represent behavioral priorities in multiple spatial reference frames. *Bioarchitecture* 3(5), 147–152. [PubMed: 24322829]
- Tartaglia MC, Zhang Y, Racine C, Laluz V, Neuhaus J, Chao L, Kramer J, Rosen H, Miller B, Weiner M, 2012 Executive dysfunction in frontotemporal dementia is related to abnormalities in frontal white matter tracts. *J Neurol* 259(6), 1071–1080. [PubMed: 22037958]
- Turken A, Whitfield-Gabrieli S, Bammer R, Baldo JV, Dronkers NF, Gabrieli JD, 2008 Cognitive processing speed and the structure of white matter pathways: convergent evidence from normal variation and lesion studies. *Neuroimage* 42(2), 1032–1044. [PubMed: 18602840]
- Wakana S, Jiang H, Nagae-Poetscher LM, van Zijl PC, Mori S, 2004 Fiber tract-based atlas of human white matter anatomy. *Radiology* 230(1), 77–87. [PubMed: 14645885]
- Waxman SG, Kocsis JD, Stys PK, 1995 *The axon : structure, function, and pathophysiology.* Oxford University Press, New York.
- Wechsler D, 1945 A Standardized Memory Scale for Clinical Use. *The Journal of Psychology* 19(1), 87–95.
- Wilson RS, Gilley DW, Bennett DA, Beckett LA, Evans DA, 2000 Person-specific paths of cognitive decline in Alzheimer's disease and their relation to age. *Psychol Aging* 15(1), 18–28. [PubMed: 10755286]

Highlights

Tract-specific WMH relate to tract-specific microstructural integrity (FA)

Tract-specific FA relates to specific cortical gray matter volumes

Combinations of tracts and cortical gray matter volumes are associated with cognition

Information processing speed relates to tract and cortical integrity

Memory relates more to cortical integrity

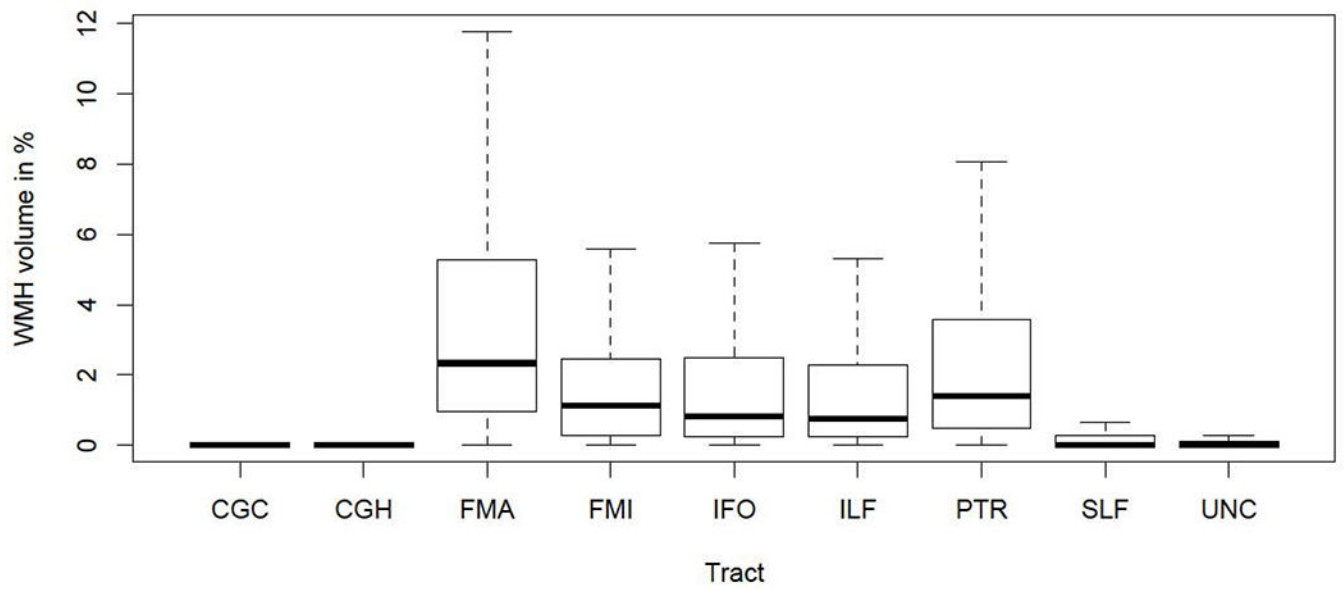


Fig.1. Boxplot of tract-specific white matter hyperintensities (WMH) ratio

Abbreviations: CGC: cingulate gyrus part of cingulum, CGH: parahippocampal part of cingulum, FMA: forceps major, FMI: forceps minor, IFO: inferior fronto-occipital fasciculus, ILF: inferior longitudinal fasciculus, SLF: superior longitudinal fasciculus, PTR: posterior thalamic radiation, UNC: uncinate fasciculus.

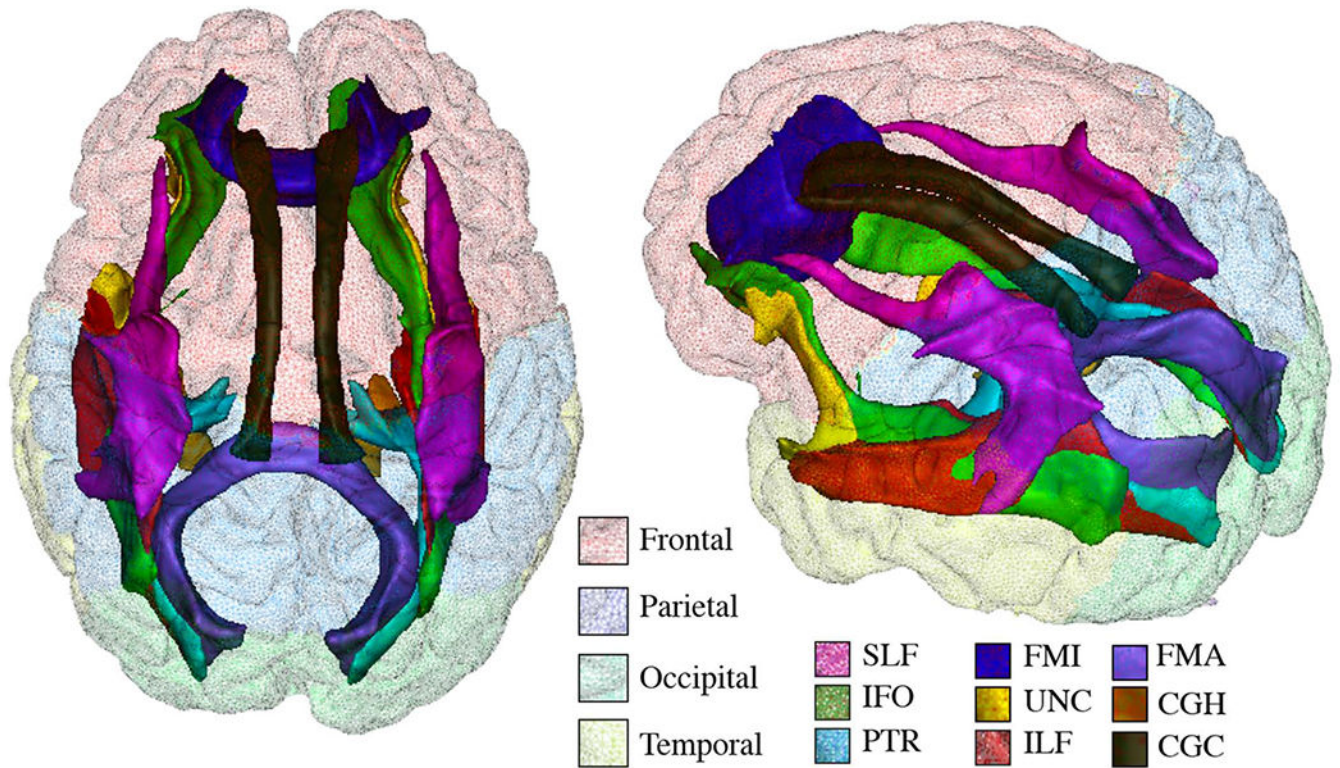


Fig.2. Composite map of white matter tracts

Composite map illustrates the frequency map (thresholded at 20%) for the nine white matter tracts, including the forceps major (FMA), forceps minor (FMI), inferior fronto-occipital fasciculus (IFO), inferior longitudinal fasciculus (ILF), posterior thalamic radiation (PTR), cingulate gyrus part of cingulum (CGC), parahippocampal part of cingulum (CGH), superior longitudinal fasciculus (SLF) and uncinate fasciculus (UNC). Colors onto the cortical surface indicate lobar regions.

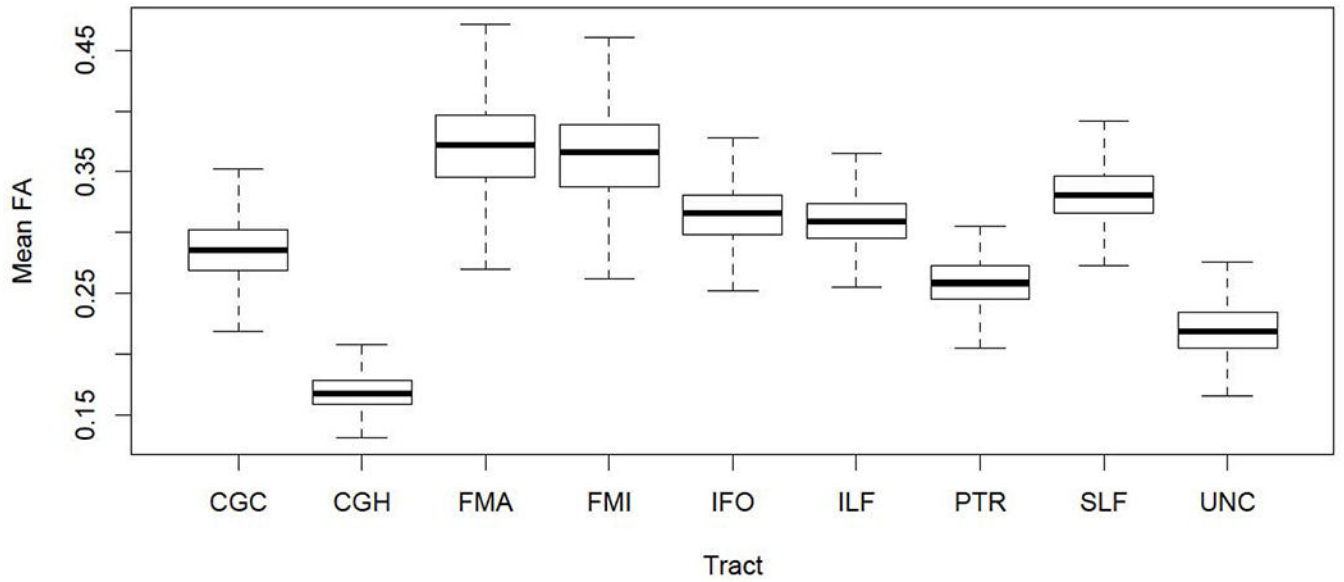


Fig.3. Boxplot of tract-specific mean fractional anisotropy (FA)

Abbreviations: CGC: cingulate gyrus part of cingulum, CGH: parahippocampal part of cingulum, FMA: forceps major, FMI: forceps minor, IFO: inferior fronto-occipital fasciculus, ILF: inferior longitudinal fasciculus, SLF: superior longitudinal fasciculus, PTR: posterior thalamic radiation, UNC: uncinate fasciculus.

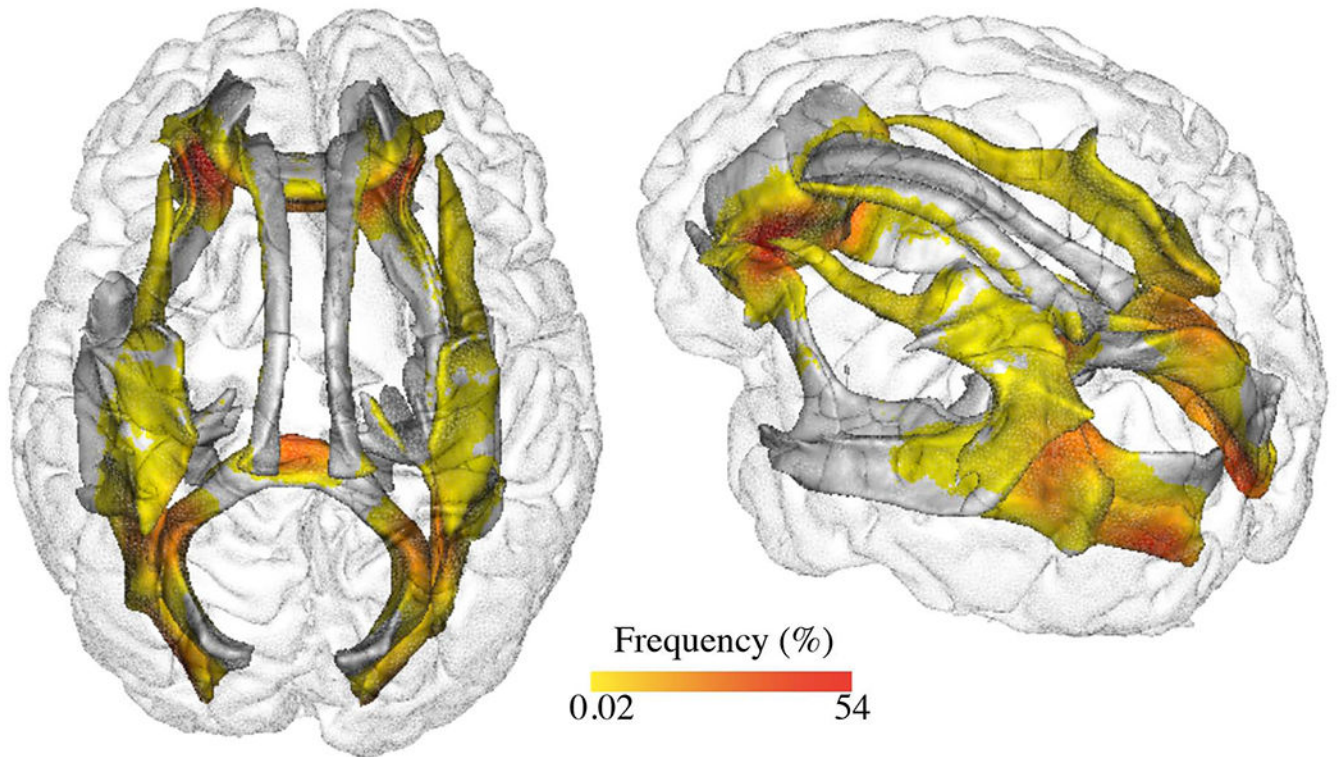


Fig. 4. Percentage of individuals with white matter hyperintensities at a voxel location
Spatial distribution of white matter hyperintensities in the study sample among nine different tracts including the forceps major (FMA), forceps minor (FMI), inferior fronto-occipital fasciculus (IFO), inferior longitudinal fasciculus (ILF), posterior thalamic radiation (PTR), cingulate gyrus part of cingulum (CGC), parahippocampal part of cingulum (CGH), superior longitudinal fasciculus (SLF) and uncinate fasciculus (UNC).

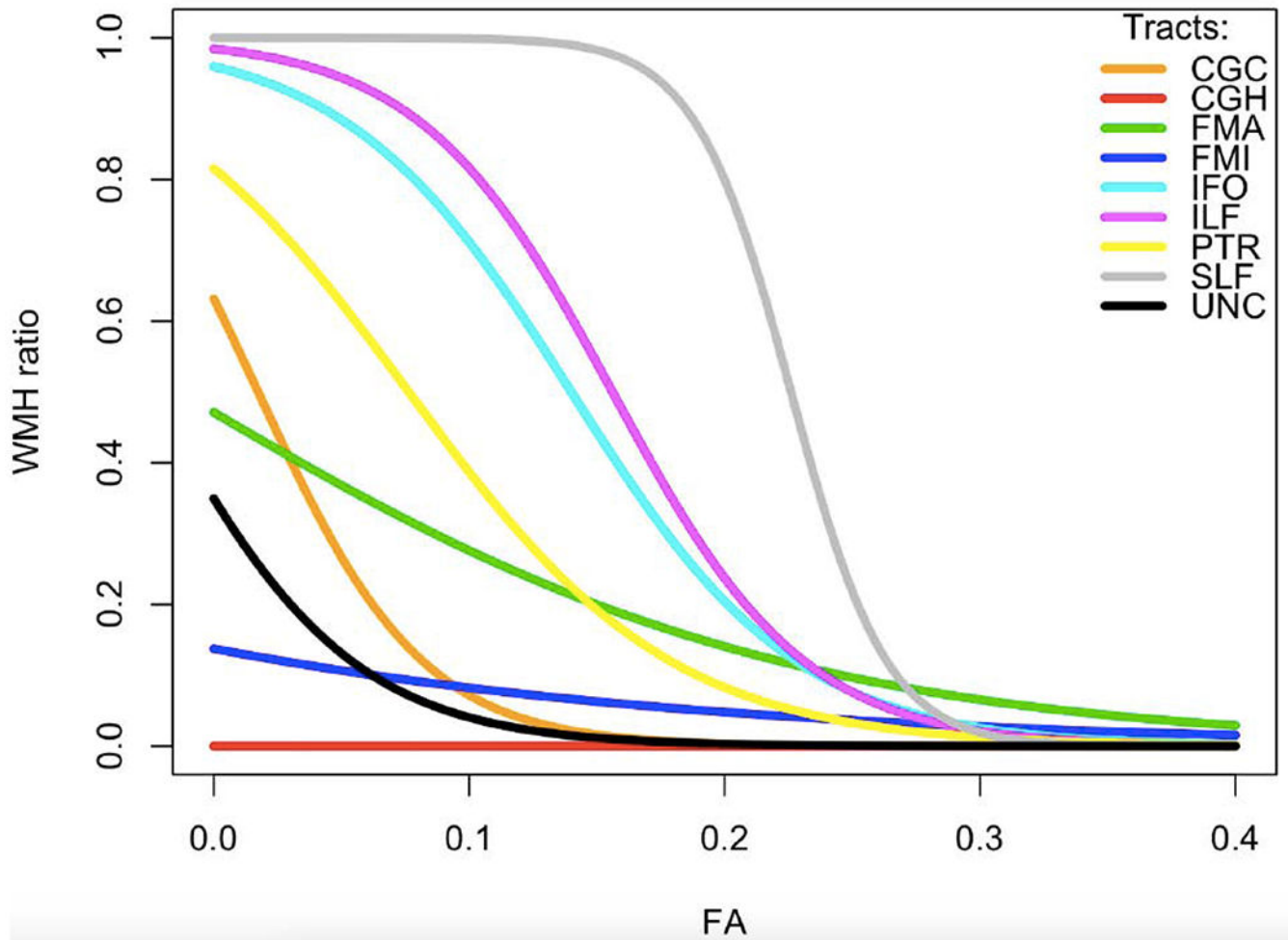


Fig.5. Logistic regression curves.

Logistic regression curves relating tract-specific mean fractional anisotropy (FA) and white matter hyperintensities (WMH) ratio within the following tracts: CGC: cingulate gyrus part of cingulum, CGH: parahippocampal part of cingulum, FMA: forceps major, FMI: forceps minor, IFO: inferior fronto-occipital fasciculus, ILF: inferior longitudinal fasciculus, SLF: superior longitudinal fasciculus, PTR: posterior thalamic radiation, UNC: uncinete fasciculus.

Table 1

Subject characteristics

| | mean/median/N | SD | Range/IQR |
|---|---------------|--------|------------------|
| Age (y) | 71.70 | 7.71 | 50.73; 91.52 |
| Gender (male) | 283 | NA | NA |
| Systolic Blood Pressure (mmHg) | 125.40 | 14.98 | 88.00; 196.00 |
| Fasting blood glucose (mg/dl) | 102.10 | 19.24 | 69.00; 273.00 |
| Total cranial volume (mm ³) | 1413.01 | 138.11 | 1063.19; 1899.36 |
| Total white matter hyperintensities volume (cm ³) | 5.45 | NA | 2.38; 10.86 |
| Overall mean fractional anisotropy ($\times 10^{-3}$ mm/s ²) | 0.32 | 0.02 | 0.24; 0.46 |

Continuous data are presented as mean, standard deviation (SD) and range when normally distributed and as median and interquartile range (IQR) otherwise. Categorical variables are shown as N.

Table 2

Tract-specific fractional anisotropy and white matter hyperintensities ratio distribution and association

| Tract | FA | | WMH ratio (%) | | | Odds Ratio |
|-------|------|-------|---------------|------|--------|-----------------------------|
| | Mean | SD | Mean | SD | Median | |
| CGC | 0.29 | 0.025 | 0.03 | 0.25 | 0 | 1.95 (<0.001) [1.8; 2.11] |
| CGH | 0.17 | 0.016 | 0.01 | 0.06 | 0 | 0.71 (<0.001) [0.634; 0.80] |
| FMA | 0.37 | 0.039 | 3.94 | 4.57 | 2.34 | 1.21 (<0.001) [1.2; 1.21] |
| FMI | 0.36 | 0.040 | 1.94 | 2.75 | 1.12 | 1.09 (<0.001) [1.08; 1.1] |
| IFO | 0.32 | 0.024 | 2.09 | 3.31 | 0.82 | 1.55 (<0.001) [1.54; 1.56] |
| ILF | 0.31 | 0.022 | 1.84 | 2.82 | 0.75 | 1.59 (<0.001) [1.58; 1.6] |
| PTR | 0.26 | 0.021 | 2.85 | 3.92 | 1.40 | 1.30 (<0.001) [1.29; 1.3] |
| SLF | 0.33 | 0.025 | 0.87 | 3.70 | 0 | 4.01 (<0.001) [3.97; 4.04] |
| UNC | 0.22 | 0.022 | 0.22 | 0.68 | 0 | 1.33 (<0.001) [1.3; 1.37] |

Descriptive statistics for tract-specific fractional anisotropy (FA) and white matter hyperintensities (WMH) ratio in the sample. Odds ratio (p value) [95%CI] corresponds to the odds of increase in WMH ratio unit associated with a unit decrease in standardized FA. SD: standard deviation, CGC: cingulate gyrus part of cingulum, CGH: parahippocampal part of cingulum, FMA: forceps major, FMI: forceps minor, IFO: inferior fronto-occipital fasciculus, ILF: inferior longitudinal fasciculus, SLF: superior longitudinal fasciculus, PTR: posterior thalamic radiation, UNC: uncinat fasciculus.

Table 3

Associations between tract-specific fractional anisotropy, white matter hyperintensities (WMH), and gray matter (GM) volumes

| | Frontal | Occipital | Parietal | Temporal |
|---------------|----------|-----------|----------|----------|
| All WM | 0.12* | 0.045 | 0.03 | 0.07 |
| CGC | -0.07 | -0.15** | -0.03 | -0.12 |
| CGH | 0.16* | 0.12 | 0.14* | 0.23*** |
| FMA | 0.15* | 0.25*** | 0.05 | 0.20*** |
| FMI | 0.25*** | 0.18** | 0.20*** | 0.13 |
| IFO | 0.08 | 0.08 | 0.06 | 0.03 |
| ILF | 0.13 | 0.1 | 0.08 | 0.04 |
| PTR | 0.06 | 0.17** | -0.04 | 0.13 |
| SLF | 0.06 | 0.047 | 0.13 | -0.034 |
| FA | 0.12 | -0.00 | 0.06 | 0.20*** |
| <hr/> | | | | |
| All WM | -0.22*** | -0.10 | -0.12** | -0.07 |
| CGC | 0.03 | -0.11 | 0.01 | 0.17 |
| CGH | -0.08 | -0.04 | 0.1 | 0.28 |
| FMA | -0.15 | -0.22** | -0.05 | -0.05 |
| FMI | -0.06 | 0.04 | -0.00 | 0.01 |
| IFO | -0.10 | -0.06 | -0.10 | -0.04 |
| ILF | -0.09 | 0.02 | -0.10 | -0.06 |
| PTR | -0.04 | 0.11 | 0.02 | 0.01 |
| SLF | -0.13 | -0.01 | -0.1 | -0.03 |
| WMH | UNC | -0.16 | -0.01 | -0.18 |
| | | | | -0.15 |

Statistics of the linear regression including lobar gray matter (GM) volumes as dependent variable and tract-specific fractional anisotropy (FA) or tract-specific white matter hyperintensity (WMH) ratio as independent variable. All MRI measures were formerly adjusted for age, gender, total cranial volume, systolic blood pressure and blood glucose level. The linear regression analysis of lobar GM volumes on tract-specific FA includes overall mean FA, and the linear regression analysis of lobar GM volumes on tract-specific WMH ratios includes overall WMH burden as additional covariates. Values represent standardized regression coefficients.

*** : p value < 0.001

** : p value < 0.01

Author Manuscript

Author Manuscript

Author Manuscript

Author Manuscript

* : p value<0.05 after Bonferroni correction.

CGC: cingulate gyrus part of cingulum, CGH: parahippocampal part of cingulum, FMA: forceps major, FMI: forceps minor, IFO: inferior fronto-occipital fasciculus, ILF: inferior longitudinal fasciculus, SLF: superior longitudinal fasciculus, PTR: posterior thalamic radiation, UNC: uncinate fasciculus.

Table 4

Associations between scores of memory and processing speed and integrity-related MRI components

| | Memory | | Processing Speed | | |
|----------------------|---------|-----------|------------------|-----------|-----------|
| | LM | VR | PAS | TrA | TrB |
| Frontal | 0.042 | 0.100 | 0.021 | 0.012 | 0.050 |
| CGH | 0.058 | 0.060 | 0.082 | 0.088 | 0.084 |
| FMA | 0.026 | 0.043 | 0.084 | 0.100 | 0.076 |
| FMI | 0.026 | 0.041 | -0.071 | 0.084 | 0.059 |
| R² | 0.011 | 0.028 *** | 0.014 | 0.047 *** | 0.036 *** |
| Occipital | 0.001 | 0.058 | 0.030 | 0.040 | 0.053 |
| CGC | -0.054 | -0.006 | -0.087 | 0.044 | 0.014 |
| FMA | 0.039 | 0.046 | 0.07 | 0.089 | 0.070 |
| FMI | 0.039 | 0.045 | -0.059 | 0.073 | 0.055 |
| PTR | 0.024 | -0.003 | -0.035 | 0.088 | 0.053 |
| R² | 0.007 | 0.011 | 0.016 | 0.052 *** | 0.028 *** |
| Parietal | 0.025 | 0.140 | 0.110 | 0.051 | 0.077 |
| CGH | 0.073 | 0.075 | 0.071 | 0.110 | 0.110 |
| FMI | 0.032 | 0.052 | -0.062 | 0.110 | 0.079 |
| R² | 0.009 | 0.035 *** | 0.017 * | 0.039 *** | 0.035 *** |
| Temporal | 0.061 | 0.130 | 0.092 | 0.059 | 0.089 |
| CGH | 0.059 | 0.065 | 0.039 | 0.092 | 0.091 |
| FMA | 0.026 | 0.046 | 0.040 | 0.110 | 0.081 |
| UNC | 0.054 | 0.039 | 0.045 | 0.083 | 0.072 |
| R² | 0.018 * | 0.038 *** | 0.021 ** | 0.053 *** | 0.049 *** |

Standardized component coefficients from partial least squares regressions including cognitive performance in memory (Logical Memory (LM), Paired Associates (PAS), Visual Reproductions (VR)), and information processing speed (Trail Making Test A (TrA) and B (TrB)) as dependent variables and combination of lobar gray matter (GM) volumes and fractional anisotropy of tracts identified as associated (table 3) as independent variables. Cognitive and MRI measures were formerly adjusted for age, gender, total cranial volume, education level, systolic blood pressure and blood glucose level. R² indicates the correlation coefficient associated with the model.

*** : p value < 0.001

** : p value < 0.01

* : p value < 0.05.

CGC: cingulate gyrus part of cingulum, CGH: parahippocampal part of cingulum, FMA: forceps major, FMI: forceps minor, IFO: inferior fronto-occipital fasciculus, ILF: inferior longitudinal fasciculus, SLF: superior longitudinal fasciculus, PTR: posterior thalamic radiation, UNC: uncinate fasciculus.